4-dimensional phase contrast imaging in congenital heart disease: How we do it

Timothy C. Slesnick, M.D.; Sassan Hashemi, M.D.

Emory University School of Medicine, Children's Healthcare of Atlanta, Atlanta, GA, USA

Introduction

The field of phase contrast (PC) imaging has expanded greatly in the last 30 years. The fundamental principle that a moving nuclei will experience a phase shift when subjected to a magnetic field gradient that is proportional to the flow velocity, and thus measurement of this phase shift can allow measurement of the velocity of the nuclei [1, 2], has transformed our approach to flow quantification. Today, cardiac magnetic resonance (CMR) is the gold standard for quantification of vascular flows [3, 4]. Though initially confined to 2-dimensional (2D) measurements of either through plane or in-plane flow, the development of 4-dimensional phase contrast imaging (4D flow) was first applied to central nervous system vasculature in the late 1980's [5] and subsequently to cardiovascular blood flow in the late 1990's [6] and has opened new avenues and insights.

Two-dimensional phase contrast imaging is now a routine part of most CMR studies in pediatric and adult patients with congenital heart disease (CHD). Though options exist for both breath held and free breathing 2D PC sequences, our lab, like most, prefer to use free breathing techniques with multiple signal averages (NSA). Assessment of flow in the aorta (Ao) and main pulmonary artery (MPA) allows for quantification of systemic (Qs) and pulmonary blood flow (Qp). Flow in the right pulmonary artery (RPA) and left pulmonary artery (LPA) allows quantification of differential pulmonary blood flow, as well as validation of the MPA flow.

In the present work, we delineate our current practices with 4D flow imaging in children[1] and young adults with CHD, with a focus on practical tips for users to bring this technology to their programs and their patients. Illustrative cases are given with some of the ever-expanding array of applications for this technology. Finally, several recent advances are highlighted which promise to continue to evolve this new technique.

Works in progress 4D Flow

The fundamental tenants of 4D flow are flow encoding in all three directions (x, y, z-axes). True 4D flow sequences obtain a 3D volume, with the fourth dimension representing time. The works in progress (WIP) 4D flow pulse sequence[2] we currently utilize is WIP 785A, first released in January of 2016 (Figures 1A and 1B, Clip 1 – to access the .avi's please visit www.siemens.com/4Dflow). The sequence utilizes 3D Cartesian sampling with flow encoding and generalized auto-calibrating partially parallel acquisition (GRAPPA) acceleration where the reference lines are acquired separately (aka ePAT). Acceleration can be applied in both phase encoding and the partition encoding directions since the dataset is a true 3D volume, with the expected decrease in signal to noise (SNR) of square root of each of the acceleration factors. When acceleration is applied in both phase encoding and partition encoding directions, SNR is decreased by

[1] Siemens Healthineers Disclaimer does not represent the opinion of the authors: MR scanning has not been established as safe for imaging fetuses and infants less than two years of age. The responsible physician must evaluate the benefits of the MR examination compared to those of other imaging procedures.

[2] WIP, the product is currently under development and is not for sale in the US and in other countries. Its future availability cannot be ensured.

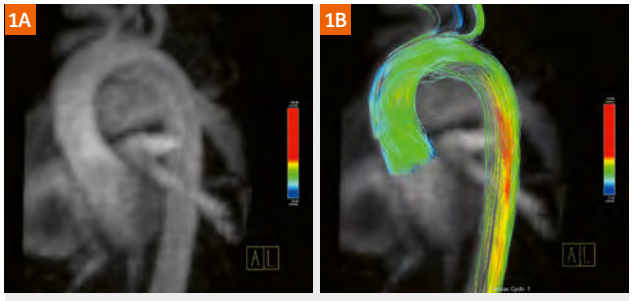

Figure 1:
4D flow magnitude **(1A)** image of an aortic arch obtained using WIP 785A, as well as particle trace image **(1B)**.

the product of those factors, but the resultant change in the geometry factor, which also influences signal to noise loss, is less pronounced than if all acceleration is performed in one direction, so acceleration of 2 x 2 does result in less signal loss than 4 x 1. One final point on acceleration is that running 4D flow sequences post-contrast will obviously result in more signal, and thus more acceleration can be applied without loss of data integrity. On our 1.5 Tesla scanner, we typically run our 4D flow sequences post contrast (if contrast is given during the routine exam), and apply ePAT in either the phase encoding direction alone with a factor of 3 or in both the phase and partition encoding directions with factors of 2 for each (2 x 2). If no contrast is given to the patients during routine exam, we typically run the 4D flow sequence applying parallel imaging with a factor of 2 in the phase encoding direction alone.

In order to obtain this quantity of data, even for a small slab of coverage, requires substantial *k*-space sampling, far longer than is possible in a breath held study. In order to minimize respiratory motion, a respiratory navigator is typically employed (though as delineated below in the product section free breathing techniques with multiple signal averages can also be used). A cross-beam respiratory navigator is positioned on the dome of the diaphragm, and an acceptance window of ± 3–5 mm is typically used (± 3 mm for smaller children, ± 4–5 mm for larger children and young adults). Some users have reported using larger respiratory navigator windows, up to ± 8 mm, with acceptable degree of motion artifacts, but we do not have personal experience with this broad a range of respiratory navigated acceptance.

The WIP sequence can be run with either prospective or retrospective gating. In patients with an irregular heart rate, it is possible to use prospective ECG gating with a reduced acquisition window to avoid data acquisition spanning into the early systolic phase of the following heartbeat. In our experience, however, we find that even with optimal modifications to the 4D flow sequences, the validity of the data due to the inherent fluctuations in the hemodynamics of patients with significant arrhythmias continues to be challenging, and typically we choose not to perform 4D Flow imaging in these patients.

Using retrospective gating, the number of reconstructed phases ("Calculated phases") can be set by the user (Figure 2). Caution should be employed, however, that the reconstructed phases will be interpolated from the true number of cardiac phases acquired, which is determined by the heart rate and the repetition time. For example, we typically acquire 3 segments per heart beat per cardiac phase, which results in a TR of 58.2 msec. In a patient with a heart rate of 75 beats per minute (bpm), and a resultant cardiac cycle of 800 msec, this would yield 13 true cardiac phases. Though the interface allows the user to set the number of reconstructed phases to any desired value, our experience has shown that using slightly less than double the number of true phases produces values which correlate well with 2D PC data. We therefore typically calculate the actual number of phases for a given patient and sequence prescription, double the value, and then

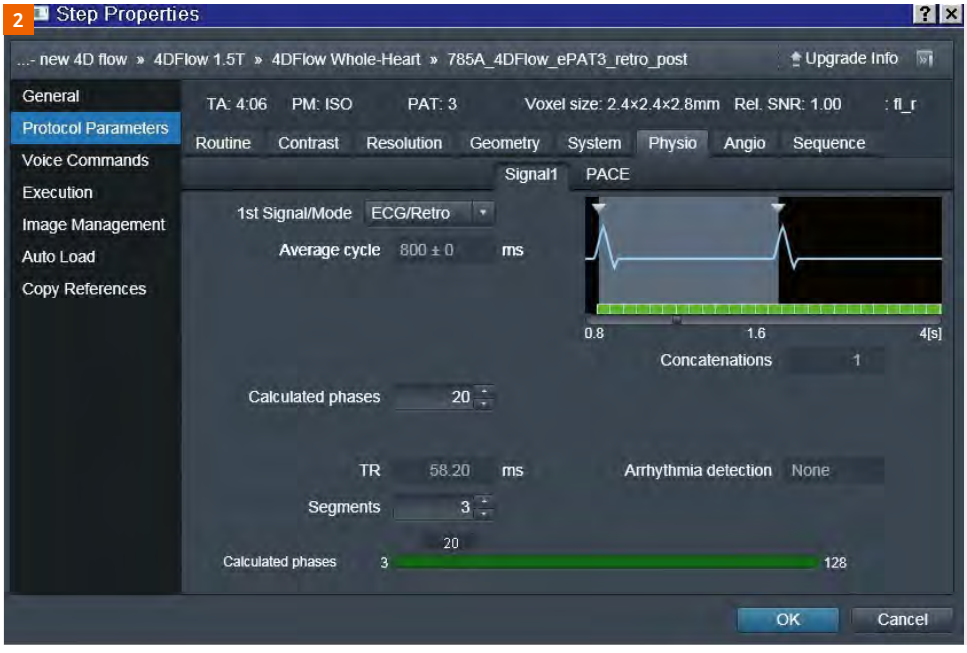

Figure 2:
Screen shot demonstrating the Physio tab on the user interface where the number of "Calculated Phases" can be adjusted and the number of true phases can be calculated (cardiac cycle length divided by the TR).

decrease slightly to allow all reconstructed phases to have some component of unique data.

Though this manipulation may seem a bit cumbersome, it allows the user to tailor the sequence and results to the individual patient. For smaller children with faster heart rates, it may be necessary to decrease the number of segments to 2 to allow a shorter TR and thus more reconstructed phases. Conversely, in older patients with slower heart rates (< 50–55 bpm) we will often increase segments to 4 to speed up the acquisition without compromising the number of reconstructed phases. Since each change to the number of segments has a direct correlation to the scan length, these manipulations must be made very thoughtfully. Increasing from 3 to 4 segments will cut acquisition time by 25%, while decreasing from 3 to 2 segments will require 50% longer. For most of our scans, we aim to reconstruct 16–25 phases, adjusting the parameters as needed.

As with any 3D dataset, obtaining isotropic voxels is advantageous as it allows the user to reformat/slice the data in any plane without loss of resolution. With the 4D Flow WIP, we typically decrease the phase and slice encoding direction percentages, so the actual obtained voxels are not quite isotropic, but the reconstructed voxels are. The user must remember that the voxel size is determined by the field of view (FOV), matrix (base resolution), and the slice thickness. FOV and matrix can be changed, but this does affect the in plane resolution and the SNR. The sequence will allow decreasing slice thickness to 1.5 mm, though in our lab we typically run the sequence at 2 mm isotropic.

Slice coverage is prescribed based on the anatomy of interest. For aortic pathology, simply covering the aortic arch (with care taken that the entirety of the aortic root, which is typically the largest portion of the thoracic aorta, is fully covered) is often sufficient. Aligning the plane in a sagittal oblique geometry along the long axis of the arch allows maximal coverage in a minimum number of slices. Depending on the child's (and aorta's) size, this can often be accomplished in as few as 12–14 slices, though with more dilated aortas 16–20 slices may be necessary. For alternative underlying pathologies, coverage may be needed for the entire ventricular volumes (when heart failure or inflow/outflow assessment is desired), branch pulmonary arteries (for TOF and single ventricle [SV] patients), or systemic or pulmonary veins (particularly in patients with anomalous returns). These cases often require wider coverage and thus more slices, so the balance between voxel size and acquisition time is paramount when planning these scans. For most 4D Flow datasets, we prescribe a straight or oblique sagittal plane of some type. Axial geometries can be used if only branch PA flow is desired, but coverage in the z-direction with axial slices is often quite limited unless large slabs are obtained. Coronal orientations are also possible, but will require phase encoding in the left-right direction (as opposed to anterior-posterior in sagittal or axial oblique geometries), so FOV and acquisition duration will be increased. Additionally, some analysis platforms have difficulties processing coronal 4D Flow datasets, though this can be overcome with manipulation on the user interface.

The final component we prescribe is our velocity encoding upper limits (VENC). As explained in the case examples below, we routinely set the VENC at the highest velocity value within the imaging prescription of interest to avoid aliasing. For most aortic and pulmonary artery studies we use either 150 or 200 cm/sec, unless there is known stenosis of a valve or great artery. For single ventricle studies where the bidirectional Glenn (BDG) or Fontan circuit are the primary area of interest, either 100 or 120 cm/sec is used, with the knowledge that aliasing may occur in the aorta but that is outside the primary vessels of interest (if quantification in the aorta is desired in an SV patient, then 150 or 200 cm/sec is used).

Product 4D Flow options

True 3D datasets

The current software platforms for Siemens Healthineers magnets allow the user to prescribe a 4D Flow dataset with a true 3D volume and flow encoding in all three directions using the product sequences alone (Figures 3A and 3B, Clip 2). This derivation must start with a base product sequence which utilizes prospective ECG triggering (more on this in a moment). On our magnet (MAGNETOM Avantofit on software platform *syngo* MR E11B), we have built this option from the underlying, "BEAT_FQ" sequence, though other options are possible. On *syngo* MR E11B, the current product sequence will not support a 3D acquisition

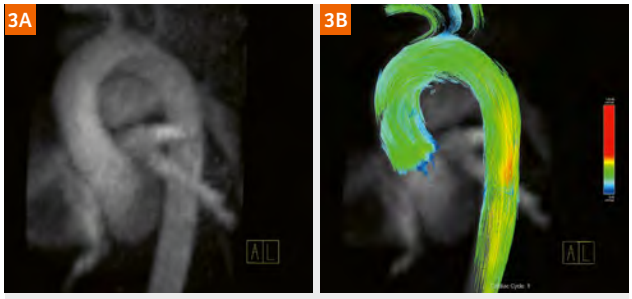

Figure 3:
4D flow magnitude **(3A)** image of an aortic arch obtained using the product 4D flow derivative, as well as particle trace image **(3B)**.

when parallel imaging with GRAPPA and reference lines obtained using "GRE/separate" (aka ePAT) is employed, so under the Resolution tab, iPAT subtab, "Integrated" must be selected to change to iPAT parallel imaging (Figure 4). On the *syngo* MR E11C and subsequent platforms 3D acquisitions are possible with ePAT image acceleration. For the product 3D acquisition, parallel imaging can only be used in the phase encoding direction. We typically run the sequence with 3 fold acceleration and perform it post-contrast to ensure adequate signal. Next, under the Sequence card, Part 1 subtab, the Dimension can be changed from 2D to 3D (for *syngo* MR E11B this option will not be available until the parallel imaging is changed from ePAT to iPAT) (Figure 5). This change will automatically convert the flow direction from "Single dir" to "Single vel" (which results in flow encoding in all three directions, represented as F>>H, Throughplane, and A>>P in a sagittal geometry) (Figure 6).

Product phase contrast sequences do not have an option for a respiratory navigator, and since data acquisition is far too long for an individual breath-hold, free breathing

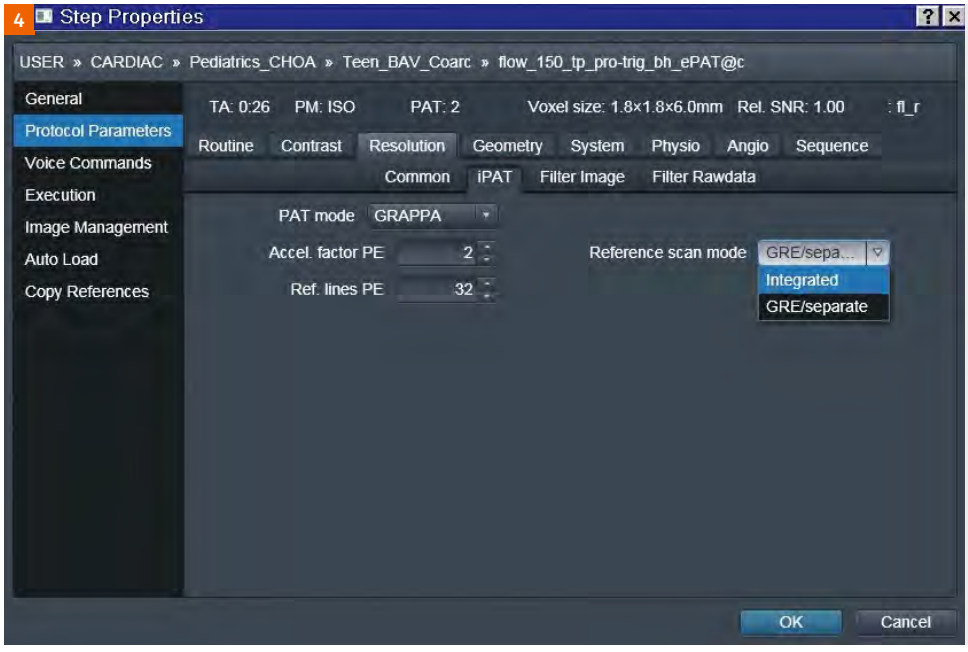

Figure 4:
Screen shot illustrating how the reference line acquisition must be changed from "GRE/separate" to "Integrated" (aka ePAT to iPAT) in order to convert the sequence as described in the text.

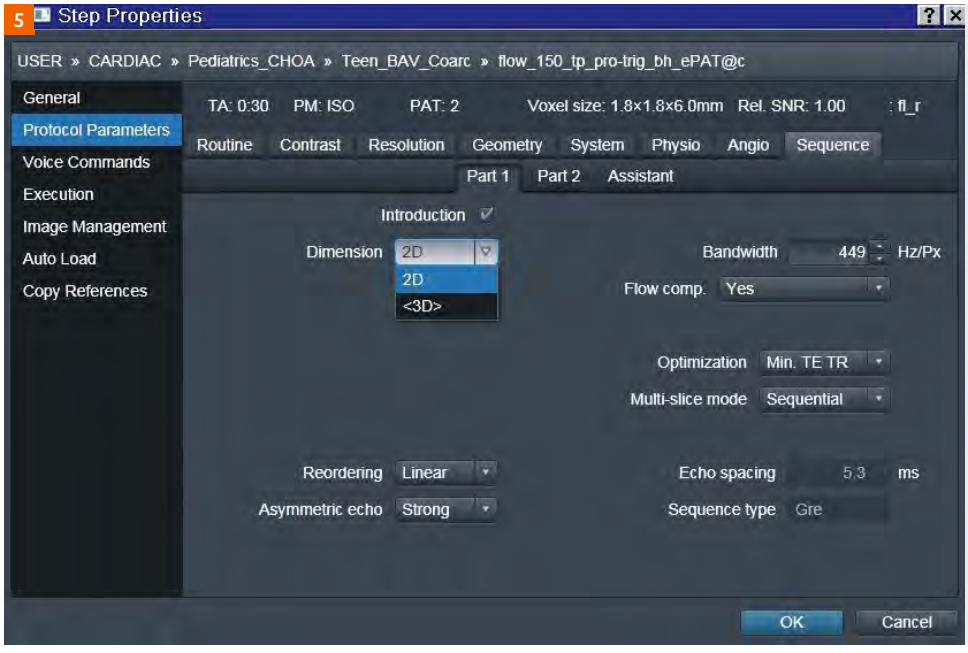

Figure 5:
Screen shot illustrating how the 2D product phase contrast sequence can be changed to a 3D volume under the Sequence tab, Part 1.

techniques with multiple signal averages are needed. Since this variant does produce a true 3D volume, it is less respiratory motion sensitive, so we typically acquire 2 NSA.

Slice thickness can be as thin as 1 mm, though again we typically run this variant at 2–2.5 mm in the interest of acquisition time. FOV and matrix are adjusted to ensure isotropic voxels. Slice orientation and number are set to cover the regions of interest. The VENC is set as described above.

The largest difference in this variant of 4D Flow is that the Siemens Healthineers current product sequence does not support retrospective gating for 3D volumes. This fact has three important consequences. First, the end of diastole cannot be captured, and thus the sequence represents only a large portion (not the entirety) of the cardiac cycle. Second, unexpected pronounced heart rate variability result in challenges with data sampling both in mistiming at the end of the cardiac cycle and missed acquisition on the beats following shorter cardiac intervals. Finally, with prospective gating, the number of phases is fixed

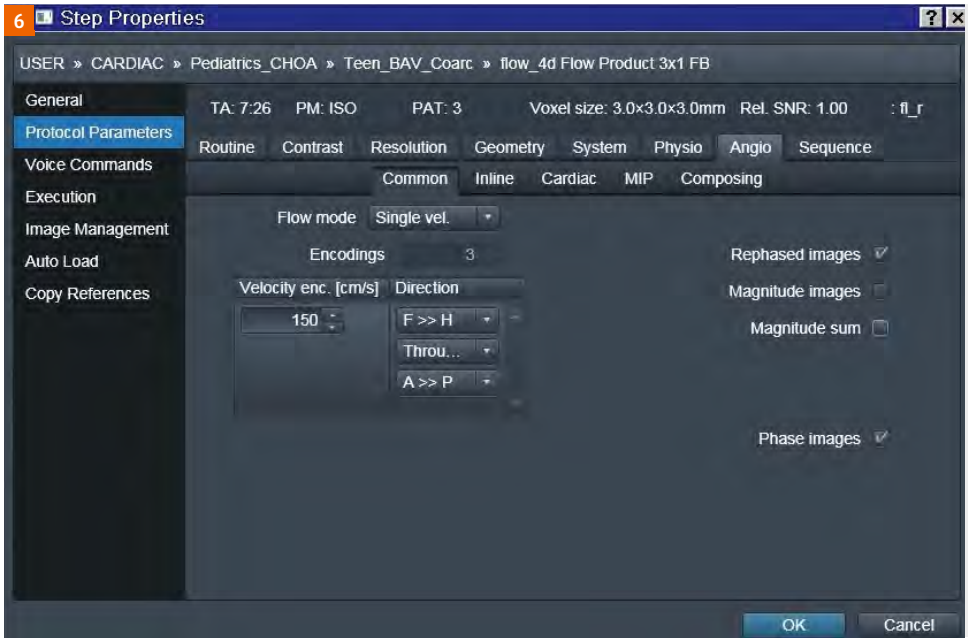

Figure 6:
Screen shot illustrating the change to the "Single vel" option with velocity encoding in all three directions (F>>H, Throughplane, and A>>P) under the Angio tab.

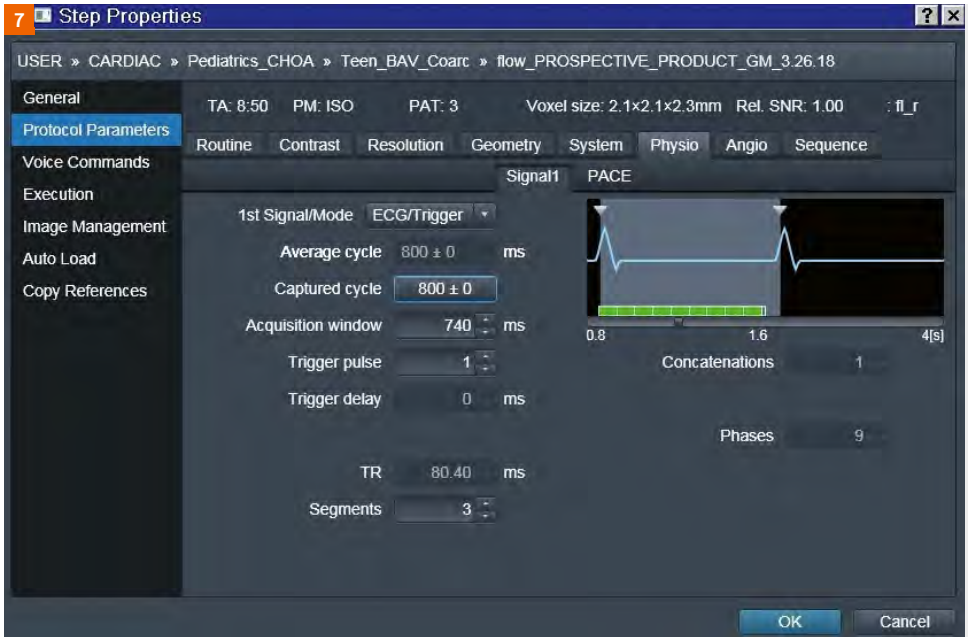

Figure 7:
Screen shot demonstrating the Physio tab on the user interface where the number of phases is displayed on the right hand side. Note, that compared to the WIP version, there is no input for "Calculated Phases" since this sequence is prospectively gated.

at the true number of acquired phases and cannot be interpolated to yield more reconstructed phases. Thus for this product 4D Flow sequence on a patient with an average heart rate of 75 bpm, a resultant cardiac cycle of 800 msec, the repetition time would be 80.4 msec (assuming 3 segments are selected) and there will only be 9 phases produced (Figure 7). If the user desires more phases, the number of segments must be reduced (with resultant increased acquisition time).

"Pseudo 4D Flow": Contiguous stack of 2D slices

An additional alternative to the product 4D Flow described above is acquisition of a contiguous stack of 2D slices, each with flow encoding in all three directions, which in summation represent a 3D volume (Figures 8A and 8B, Clip 3). The sequence can again be built starting with the base "BEAT_FQ" sequence. It is important when setting up the multiple 2D slices to utilize no slice gap (aka "Distance factor") (Figure 9). Parallel imaging can remain with "GRE/separate", and similar to the true 3D product sequence, acceleration is only possible in the phase encoding direction. We typically run the sequence post-contrast with 3 fold acceleration.

Since there is no option for respiratory navigator on the product flow sequences, again multiple signal averages are employed. As opposed to the variant described above, 2D slices are more motion sensitive, so we typically utilize 3 NSA with the patient free breathing (though with small patients and very shallow respirations, we have utilized 2 NSA with this variant).

With a contiguous stack of 2D slices, minimum slice thickness is 2.8 mm, which means that even with FOV and matrix optimization, the isotropic voxel size is larger than on other 4D flow variants. Typically, we run this variant with 3 mm isotropic voxels, which does result in decreased resolution which is readily apparent on the magnitude images (Figures 10A and 10B), but as explained below, still produces reasonable data for flow visualization and hemodynamic analysis.

Under the Angio tab, "Flow mode" can be manually changed from the standard "Single dir" to the "Single vel" (Figure 6). The VENC is set to an appropriate value.
The contiguous stack of 2D slices variant does have the advantage that it, like the WIP, can be run with retrospective gating, and thus the number of reconstructed phases can be set by the user (Figure 11). As described above, we do not recommend setting the total phases greater than twice the number of actual phases as

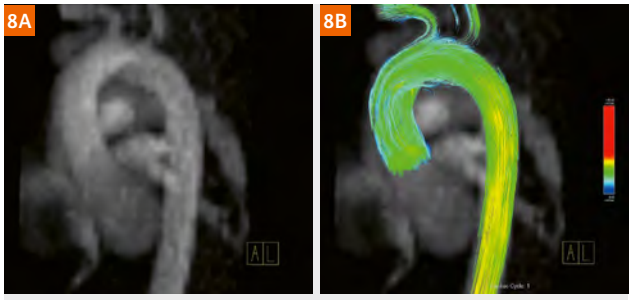

Figure 8:
4D flow magnitude **(8A)** image of an aortic arch obtained using the product "pseudo 4D flow" stack of 2D slices derivative, as well as particle trace image **(8B)**.

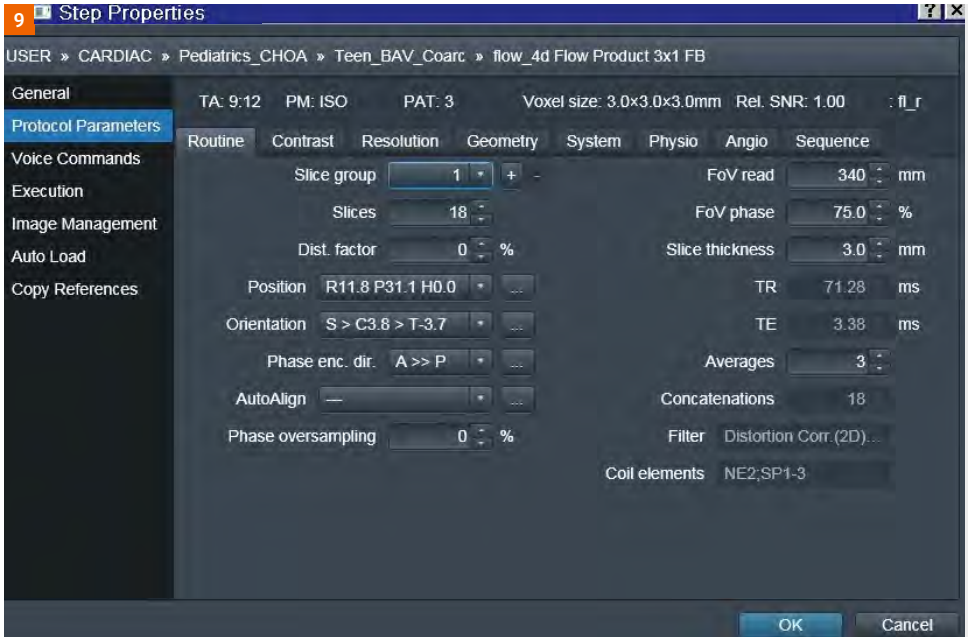

Figure 9:
Screen shot of the Routine tab where the stack of slices are composed with no gap ("Distance Factor").

determined by the repetition time and the heart rate, but you can achieve improved temporal resolution compared to the other product variant (where prospective gating is the only option).

In our experience, for similar patient's conditions and imaging data size, the continuous stack of 2D slices technique requires a shorter acquisition time than the true 3D volume product variant. This time savings does come at a price of worse spatial resolution, but offers the user improved temporal resolution compared to the other product option and also does allow retrospective gating. As described below, for flow visualization and simple quantification, we have found the resolution of this technique to be sufficient.

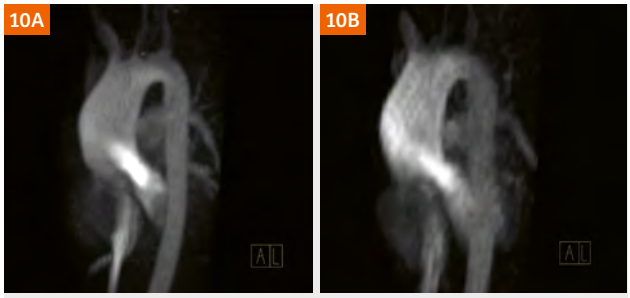

Figure 10:
Comparison of imaging on the same patient with both WIP **(10A)** and product pseudo 4D flow images **(10B)**. Note that the spatial resolution is not as good with the latter technique.

Analysis of data

Currently, we use prototype Siemens Healthineers "4Dflow v2.4" software for the majority of our 4D flow post-processing. In its current form, it is a work-in-progress software intended only for research which is equipped with good visualization and analytic options. User interface is simple and familiar since it uses the same format as in other MRI software packages in the Siemens Healthineers *syngo* ecosystem. It is divided into six consecutive tabs which guide the user from loading the data to visualization of 4D flow.

There is no PACS integration available at this time and 4D flow data should be loaded from a local disk. After loading the study ("Study Load" tab), the user can navigate between different phases and slices to find the desired structure and check for gross aliasing in different velocity encoding directions. You can also crop the dataset in phase and frequency encoding directions retrospectively (Crop Box). This helps to minimize the use of processing resources by the software, provides more accurate background phase correction and also reduces noise during visualization.

The second tab, "Corrections", provides background phase correction, anti-aliasing and motion tracking. Background phase correction extracts the stationary tissue by looking at the variance of velocities in each voxel which is deemed to be the lowest for stationary tissue. The resultant velocities in each slice are corrected so that the stationary tissue has zero velocity. As mentioned previously, cropping

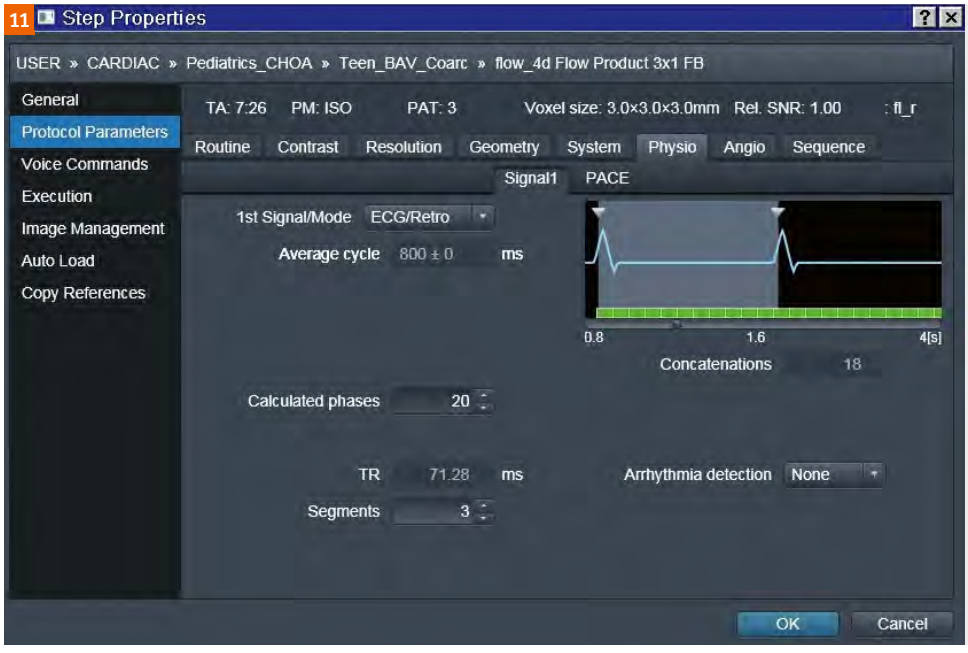

Figure 11:
Similar to Image 2, the Physio tab on the user interface with the stack of 2D slices technique gives the user the ability to input the number of "Calculated Phases".

the dataset in the previous tab helps to eliminate wrap and ghosting artifacts which may interfere with stationary tissue extraction. The anti-aliasing algorithm looks for very large opposite jumps in the velocity-time curve for each voxel and removes the wrap introduced by insufficient velocity range. Finally, motion tracking uses a symmetric deformable registration technique to track the segmented anatomy, analysis planes and particle seeds over time. Note that motion tracking requires at a minimum of 16 slices to function properly, per the Siemens Healthineers user manual. We recommend utilizing all three correction techniques to provide the most robust data.

Before proceeding to the next tab, we adjust the "segmentation threshold" from the tools tab in the bottom toolbox. This slider controls the threshold-based segmentation according to the signal intensity. The goal is to find the balance between including the desired anatomy without going beyond vessel boundary (Figure 12). After adjusting the threshold, the mesh transparency can be adjusted or turned off from the display tab if desired.

Since the majority of our 4D flow patients have complex and abnormal flow patterns (e.g. eccentric and helical flow in ascending aorta in stenotic bicuspid aortic valve or low velocity and opposing flow directions in Fontan circuit), we have opted not to use centerline and vessel model extraction available in "Segmentation" tab and skip to "Flow evaluation". These are options within the software platform and can streamline the workflow for patients with laminar flow, but for the majority of our cases this aspect of the software often produces unreliable results (Figure 13).

Next, under the "Flow evaluation" tab, there are different functions located under sub-tabs: "Planes" and "Calc". Under Planes, the user can draw contours along the vessel(s) of interest for flow quantification and particle seeding for visualization. We recommend setting the overlay to "none" for easier recognition of the anatomy (Figure 14). One can then navigate through the vessel in the 3D viewer on the left hand side of the screen. Note that contours can only be drawn in the left upper window, marked by a red border. Therefore, the red orthogonal line should always be perpendicular to the flow at the desired location. Once a contour is drawn, the flow-time curve will be automatically shown in the lower section of the screen. After all contours are added, user can switch

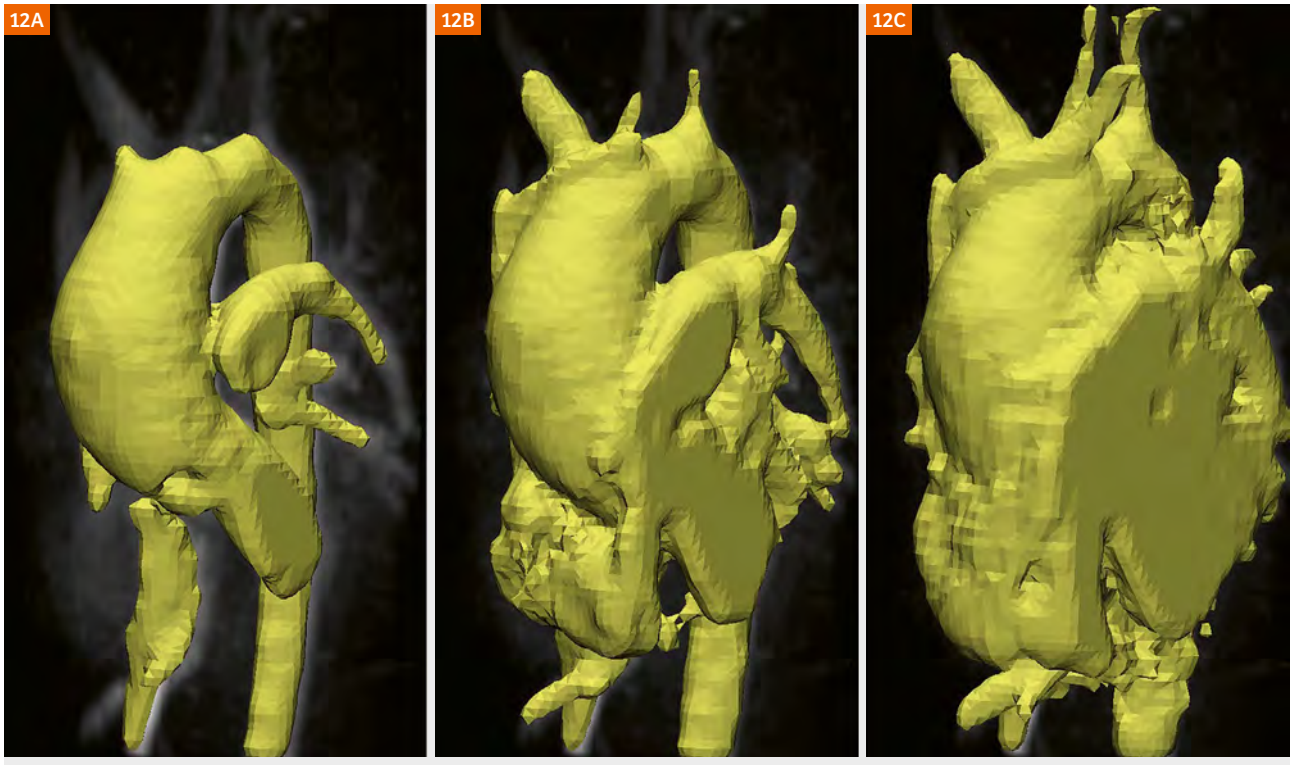

Figure 12:
Segmentation with the Threshold slider: inadequate **(12A)**, adequate **(12B)**, excessive **(12C)** threshold.

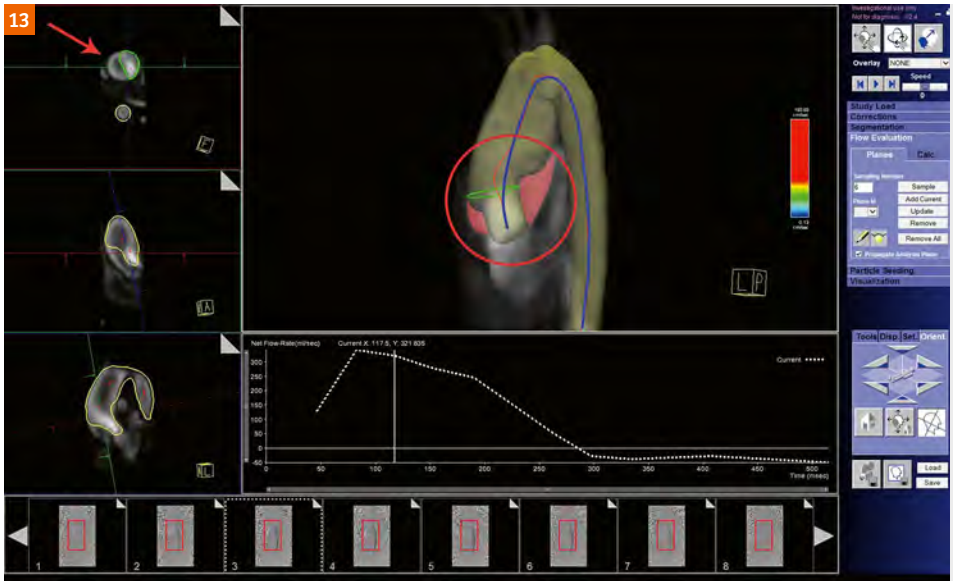

Figure 13:
Unsuccessful centerline extraction and volume segmentation in a patient with bicuspid aortic valve. The true centerline (blue) and unsegmented aortic volume (bright red) are shown. Arrow points to the unsegmented ascending aortic lumen in axial plane.

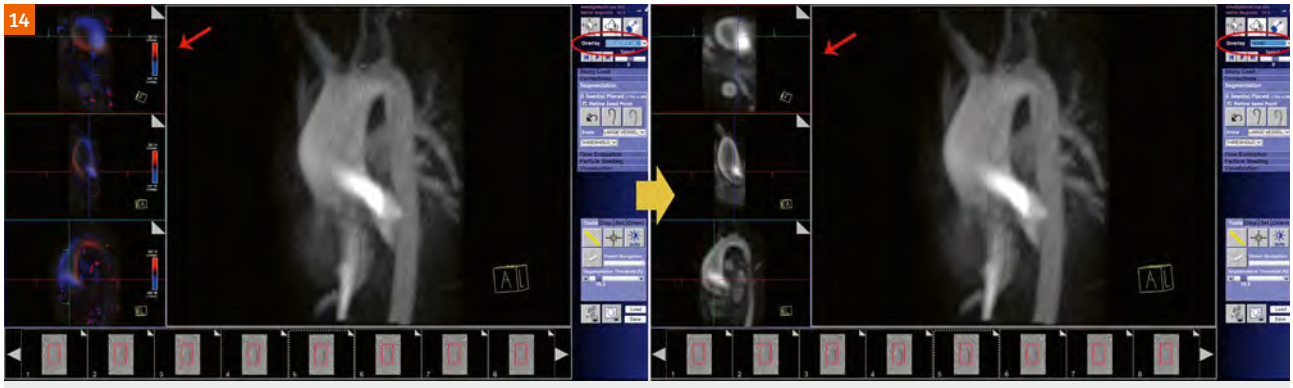

Figure 14:
Switching the overlay preset to "none" makes for easier navigation of the anatomy in the left panel (arrow).

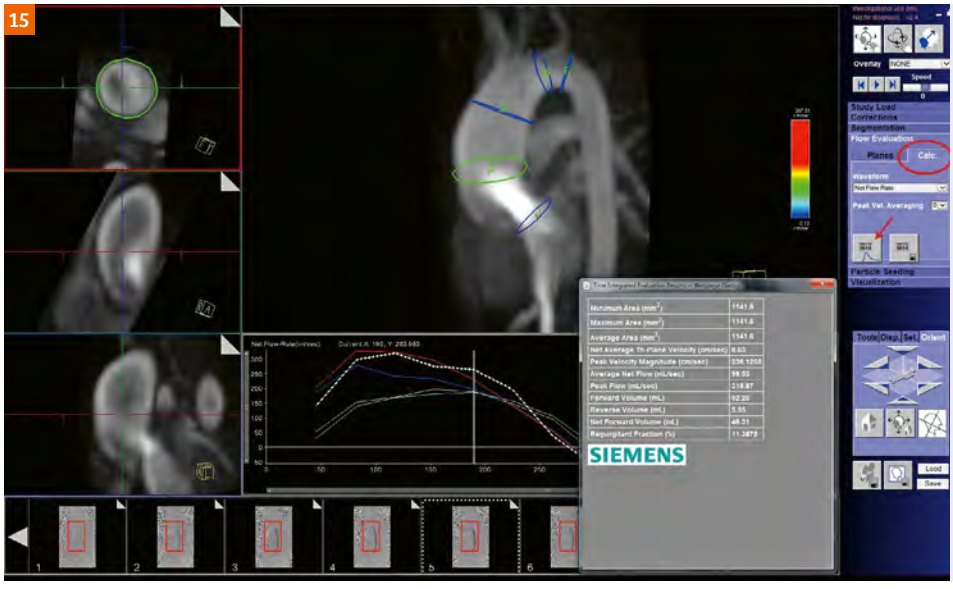

Figure 15:
Flow quantification through the desired contour by switching to the "Calc" tab in flow evaluation.

to calculation tab to get detailed flow quantification (e.g. net flow, velocities, regurgitation fraction) through each contour. This is a valuable option to cross-examine 2D phase contrast flow data with 4D flow, especially in cases when 2D flow data quality is suboptimal (Figure 15).

The focus of the last two tabs is visualization of 4D flow. The "Particle seeding" tab allows the user to seed each contour drawn in the previous step with either the same or different colors (up to 4 colors). In cases where there are multiple inflows, the user can assign different colors to better visualize flow contribution and behavior during mixing (e.g. color coding SVC and IVC in Fontan circuit or pulmonary veins and mitral regurgitation jet in mitral valve disease). The user can also choose between seeding the drawn contours or the entire segmented volume by switching between volume and planes in the drop down menu. There are options to control the density of particle seeds, intervals in which they are emitted and the number of cardiac cycles they are visualized throughout. In our lab, we typically only change particle density for better visualization. In general, we use higher density in cases with larger voxel size (50–60% for 2–2.5 mm voxels and 70-80% for 2.6–3 mm voxels).

The final tab offers three visualization options. "Vector Field" illustrates the velocity vectors summation in the segmented planes or volume for each voxel over the cardiac cycle. "Particle Traces" continuously creates time-resolved pathlines originating from the seed planes to visualize the dynamic change in trajectory and velocity. "Streamlines" captures the instantaneous 3D velocity vector field in each cardiac phase. Unlike "Particle Traces", it does not represent temporal evolution of flow in the vessel (Figure 16). We prefer to visualize our 4D flow data with "Particle Traces" since subjectively it is more easily understood (and has good agreement with "Streamline" visualization). Finally, the user can export desired images or movie clips or save the workflow (segmentation, centerline and contours) for future use.

Case examples

Our most common patient population in which we utilize 4D flow imaging is those with various forms of Aortopathies. Bicuspid aortic valve patients frequently have abnormal flow jets in the ascending aorta, and in extreme examples can have a left hand helix pattern (Figure 17, Clip 4). Those with genetic syndromes, such as Turner syndrome, may have vortex formations in atypical locations, such as at the base of the left subclavian artery at the terminal end of an elongated transverse arch (Figure 18, Clip 5). There is work underway to assess these abnormal flow patterns and the resultant effect on wall integrity, rate of vascular dilation, and propensity to dissection [7–9]. Using the tools we have described above, flow dynamics can be visualized and basic assessment of hemodynamics can be obtained. Calculation of wall shear stress can also be performed. In our lab, when patients are found to have altered flow patterns in various forms of Aortopathy, the frequency of their follow up is often increased, and consideration is given for how these insights help predict their risk of cardiovascular events in the scope of surgical timing and planning.

The next most common patient population is those with repaired tetralogy of Fallot (TOF). Regardless of whether a transannular patch is used at the time of TOF repair, the

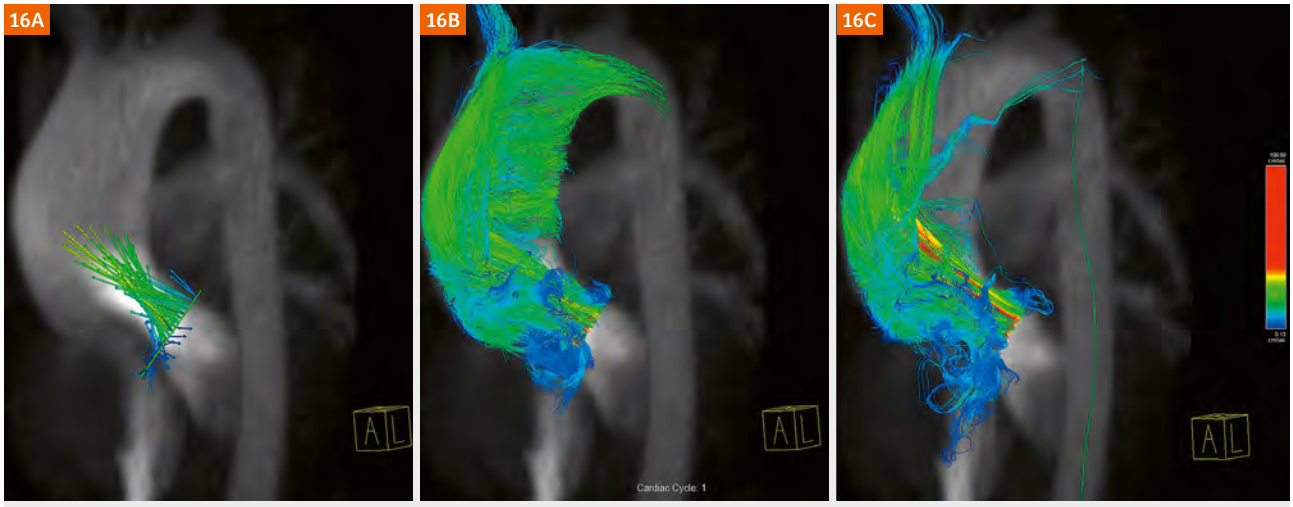

Figure 16:
Visualization options: vector field **(16A)**, particle traces **(16B)** and Steamlines **(16C)**.

pulmonary valve is virtually always non-functional by the time patients reach adolescence, and severe pulmonary insufficiency (coupled often with some degree of residual obstruction) is nearly universal. Visualization of the flow in the RVOT, both stenotic and regurgitant, is very helpful to understand the progression of the disease (Figure 19, Clip 6). Flow within the main and branch PA's, with quantification of vortices, can be studied and correlated with presence and rate of RV dilation [10–12]. In those with irregular main and branch pulmonary artery architecture, such as those with pseudoaneurysm formation, these abnormal flow patterns are even more pronounced (Figure 20, Clip 6).

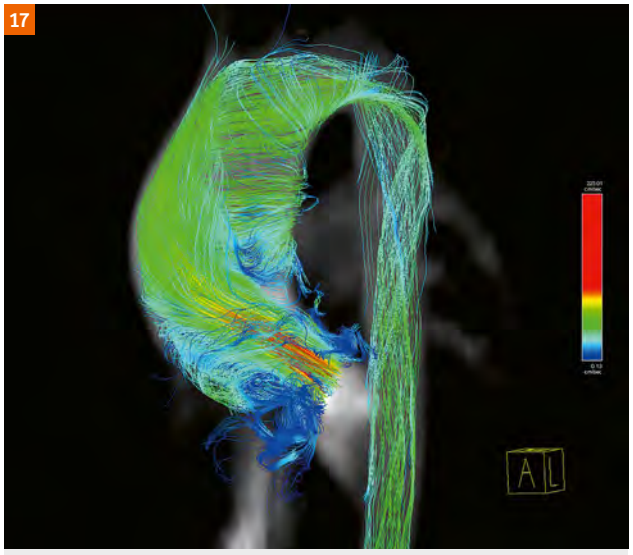

Figure 17:
Patient with a bicuspid aortic valve and a left hand helical pattern in the ascending aorta.

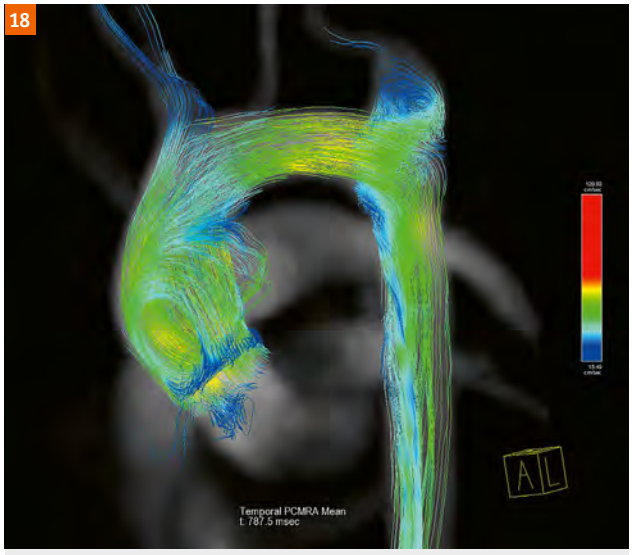

Figure 18:
Patient with Turner syndrome, no evidence of coarctation of the aorta, but with a prominent vortex formation at the base of the left subclavian artery.

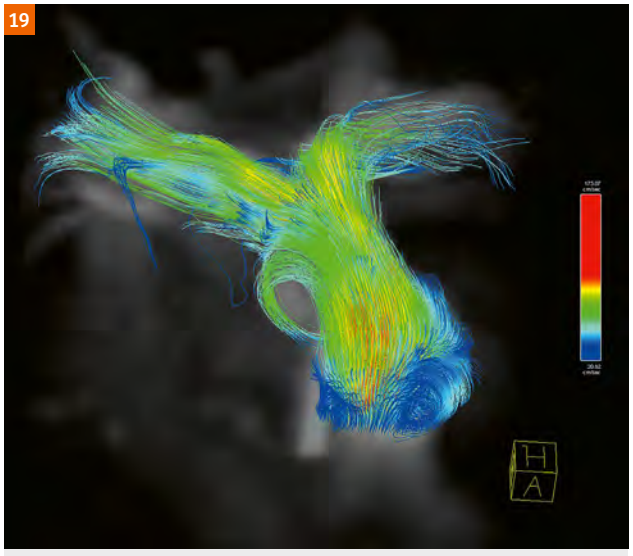

Figure 19:
Patient with repaired tetralogy of Fallot and turbulent flow noted in the main and branch pulmonary arteries.

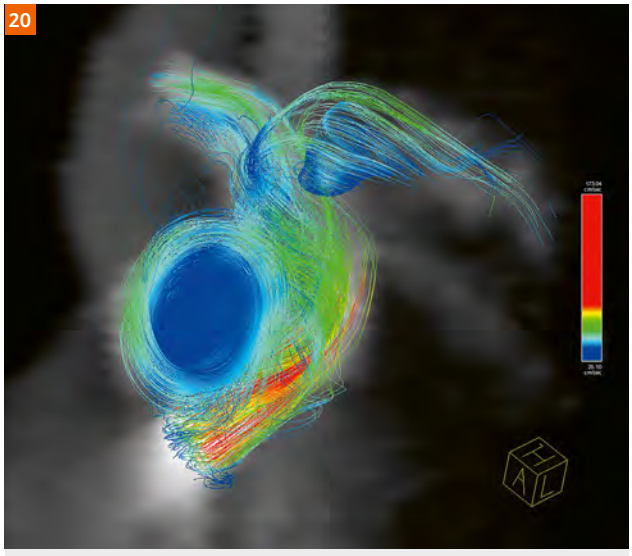

Figure 20:
Different patient with repaired tetralogy of Fallot and a pseudoaneursym on the anterior surface of the main pulmonary artery. Note the prominent vortex within the pseudoaneurysm.

In our opinion, one of the most helpful patient subgroups for 4D flow imaging are those with single ventricle anatomies. A heterogeneous group, ranging from variants such as tricuspid atresia with a single left ventricle, to those with hypoplastic left heart syndrome with a single right ventricle, to those with heterotaxy syndrome with a myriad of systemic and pulmonary venous anomalies on top of their intracardiac defects, these patients truly represent the extreme end of complexity in the field of congenital heart disease. The unifying feature for these patients is the series of staged palliations they undergo, culminating in a Fontan procedure. With only a single functional ventricle which must be used to pump blood to the body, the Fontan circulation relies on passive systemic venous return into the pulmonary arteries by anastomosing the superior vena cava (SVC) (Figure 21, Clip 7) directly to the PA and connecting the inferior vena cava (IVC) to the PA as well (Figure 22, Clip 8), via either an intracardiac tunnel or a separate conduit.

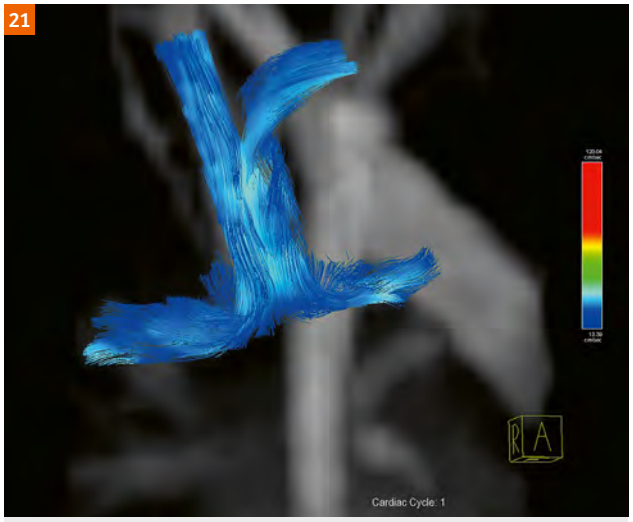

Figure 21:
Flow from the superior vena cava into the branch pulmonary arteries in a patient with single ventricle anatomy who has undergone a bidirectional Glenn anastomosis.

In patients whom have undergone a Fontan completion, altered flow hemodynamics within their circuit can lead to several clinical issues. One of the most difficult to assess is formation of pulmonary arteriovenous malformations (PAVM), thought to be due to lack of a component of hepatic blood flow (termed “hepatic factor”) to reach the pulmonary capillary bed in affected lung segments. Knowledge of the streaming of the inferior systemic venous return, therefore, is of paramount importance in assessing these patients’ risk for development of PAVM’s [13]. Traditional 2D flow imaging can assess total volumes of flow into the RPA and LPA, but cannot quantify how much of each lung’s arterial supply comes from the IVC versus the SVC. While the Siemens Healthineers software mentioned above does not have specific features to

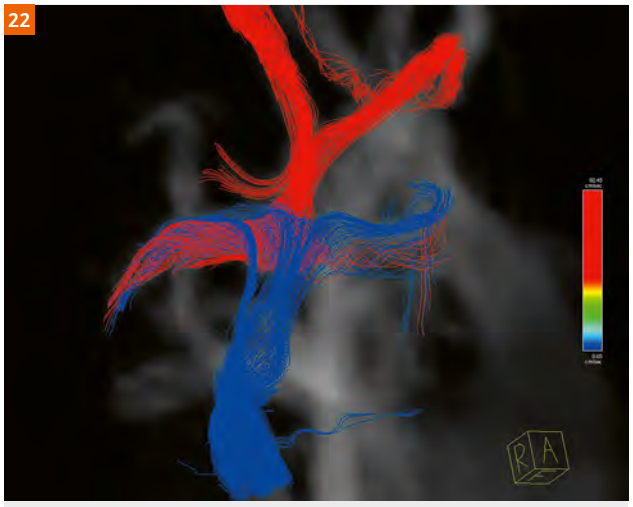

Figure 22:
Flow from the superior vena cava (colored red) and inferior vena cava (labeled blue) into the branch pulmonary arteries in a patient with single ventricle anatomy who has undergone a bidirectional Glenn anastomosis and subsequent Fontan completion. In this patient’s case, there was a small fenestration placed in the Fontan baffle, seen by the blue streamlines heading rightward on the image near the lower margin of the Fontan.

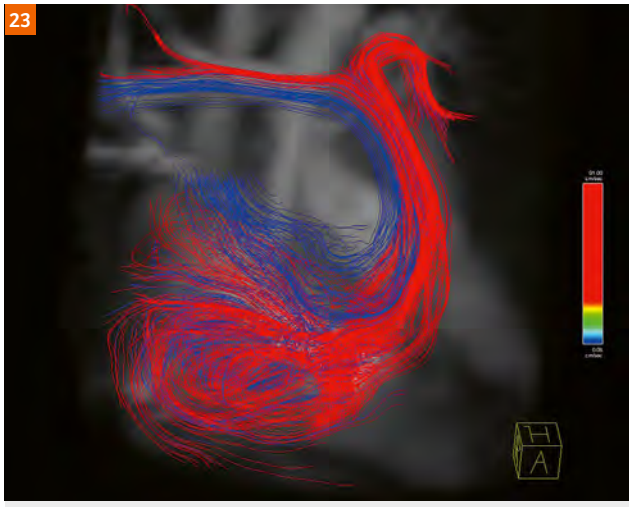

Figure 23:
Patient with Ebstein’s anomaly of the tricuspid valve, with flow across the superior aspect of the tricuspid valve labeled blue and across the inferior aspect labeled red, so that the abnormal flow in the right ventricle based on portion of tricuspid inflow can be visualized.

quantify flow volumes produced only from select vessels, we have developed an in-house MATLAB code which allows us to perform these calculations.

One final application that we are increasingly using 4D flow to assess is intraventricular flow dynamics in patients with heart failure or abnormal ventricular loading. While in adult patients, this topic is much more common in those with a structurally normal heart and heart failure from ischemic cardiac disease [14], in pediatric patients many forms of native and palliated congenital heart disease lead to long-term heart failure. Labs have looked at both left and right ventricular mechanics, including in patients with repaired TOF [15] and single ventricle patients [16, 17]. An additional, less studied disease type is patients with Ebstein's anomaly, where marked tricuspid insufficiency results in very abnormal flow patterns in the right ventricle (Figure 23, Clip 9). Performing 4D flow allows visualization of these hemodynamics, which may lead to better understanding of the mechanism of ventricular dilation and dysfunction for many of these patients.

Future directions

One limitation of 4D flow is the long acquisition times required. With the addition of compressed sensing and other image acceleration techniques, data acquisition times continue to shrink, allowing increases in spatial and temporal resolution in the datasets. Many vendors and labs are now working towards a vision of having 4D flow represent a "one stop shop" for congenital cardiac magnetic resonance imaging. One can imagine that if the spatial resolution can be decreased to roughly one millimeter voxels, then full anatomic reconstructions including short axis cine stacks can be extracted from the 4D datasets for analysis. If the temporal resolution can be improved to match current 2D flow methodologies (typically 30 phases per cardiac cycle), and retrospective gating acquisitions are used, then the 4D flow data would obviate the need for additional 2D phase contrast imaging. Thus, a high spatial and temporal resolution 4D flow dataset would provide all of the anatomic, functional, and flow data on a given patient, without need for acquiring separate double oblique 2D planes. This approach also has the advantage of being much easier for a technologist to acquire, as it is not patient specific / anatomy dependent for accurate image plane set up.

There are, however, several existing challenges to such an approach. Full chest coverage with millimeter voxels requires a large quantity of data, and this is amplified by the desire for high temporal resolution increasing the number of phases. For example, in many adolescent size patients, in order to cover the whole chest in a sagittal geometry with 1 mm slices, 100–150 slices are needed. If temporal resolution of 30 phases per cycle is desired, this will produce between 12,000 and 18,000 images. This vast array of data takes substantial time for reconstruction, made even more computationally demanding when iterative reconstruction is used with compressed sensing. Computational power and processors continue to improve, but most labs that are currently taking this type of approach to 4D flow imaging the reconstruction is done off-line and takes several hours before the data is ready.

Another challenge to this approach to 4D flow imaging is ensuring consistent, uniform signal throughout the study. As discussed above, while 4D flow sequences can be obtained with or without contrast, performing these sequences post-contrast allows increased SNR and CNR as well as higher degrees of parallel imaging acceleration. In the past, blood-pool gadolinium contrast agents such as Gadofosveset trisodium were used in several pediatric labs for performance of contrast enhanced MR angiography and 4D flow imaging [18], but this agent is no longer commercially available in the United States. Another option is non-gadolinium based contrast agents, such as ferumoxytol, which has been used for neonatal and pediatric CMR studies, though our lab does not have personal experience with this approach. Ferumoxytol has a different risk profile than gadolinium based agents, but there is data that for select patient groups these techniques can decrease the need for sedation/anesthesia (which also carries its own inherent risks) [19].

Conclusions

Application of 4D flow imaging to patients with congenital heart disease is an exciting new avenue for greater understanding of patient specific hemodynamics. Both prototype sequences as well as derivations of product pulse sequences allow acquisition of 4D flow datasets, with strengths and weaknesses in each technique. In our lab, we utilize a combination of these sequences, tailored to the individual patient anatomy, size, heart rate, and time limitations on the study. While several third party analysis platforms are available, at the current time the majority of our experience is with the Siemens 4D flow software, and we find that both the 3D visualization and quantification potential on this platform allows comprehensive use of these 4D flow data for our patients.

To access the .avi clips please visit

www.siemens.com/4Dflow

Abbreviations

2D	2-dimensional	**GRAPPA**	Generalized auto-calibrating partially parallel acquisition	**Qp**	Pulmonary blood flow
4D flow	4-dimensional phase contrast imaging			**RPA**	Right pulmonary artery
Ao	Aorta	**IVC**	Inferior vena cava	**PC**	Phase contrast
bpm	Beats per minute	**LPA**	Left pulmonary artery	**TR**	Repetition time
BAV	Bicuspid aortic valve	**MPA**	Main pulmonary artery	**SNR**	Signal to noise ratio
BDG	Bidirectional Glenn	**NSA**	Number of signal averages	**SV**	Single ventricle
CMR	Cardiac magnetic resonance imaging	**PAVM**	Pulmonary arterio-venous malformations	**SVC**	Superior vena cava
				Qs	Systemic blood flow
CHD	Congenital heart disease			**TOF**	Tetralogy of fallot
FOV	Field of view	**PA**	Pulmonary artery	**VENC**	Velocity encoding
				TOF	Tetralogy of fallot
				VENC	Velocity encoding

References

1 P. R. Moran. "A flow velocity zeugmatographic interlace for NMR imaging in humans". Magn Reson Imaging, 1, 197-203, 1982.
2 M. O'Donnell. "NMR blood flow imaging using multiecho, phase contrast sequences". Med Phys, 12, 59-64, 1985.
3 A. J. Powell and T. Geva. "Blood flow measurement by magnetic resonance imaging in congenital heart disease". Pediatr Cardiol, 21, 47-58, 2000.
4 K. K. Whitehead, K. S. Sundareswaran, W. J. Parks, M. A. Harris, A. P. Yoganathan and M. A. Fogel. "Blood flow distribution in a large series of patients having the Fontan operation: a cardiac magnetic resonance velocity mapping study". J Thorac Cardiovasc Surg, 138, 96-102, 2009.
5 C. L. Dumoulin, S. P. Souza, M. F. Walker and W. Wagle. "Three-dimensional phase contrast angiography". Magn Reson Med, 9, 139-149, 1989.
6 H. G. Bogren and M. H. Buonocore. "4D magnetic resonance velocity mapping of blood flow patterns in the aorta in young vs. elderly normal subjects". J Magn Reson Imaging, 10, 861-869, 1999.
7 L. Mirabella, A. J. Barker, N. Saikrishnan, E. R. Coco, D. J. Mangiameli, M. Markl and A. P. Yoganathan. "MRI-based Protocol to Characterize the Relationship Between Bicuspid Aortic Valve Morphology and Hemodynamics". Ann Biomed Eng, 43, 1815-1827, 2015.
8 N. Saikrishnan, L. Mirabella and A. P. Yoganathan. "Bicuspid aortic valves are associated with increased wall and turbulence shear stress levels compared to trileaflet aortic valves". Biomech Model Mechanobiol, 14, 577-588, 2015.
9 Y. Shan, J. Li, Y. Wang, B. Wu, A. J. Barker, M. Markl, C. Wang, X. Wang and X. Shu. "Aortic shear stress in patients with bicuspid aortic valve with stenosis and insufficiency". J Thorac Cardiovasc Surg, 153, 1263-1272 e1261, 2017.
10 J. Geiger, M. Markl, B. Jung, J. Grohmann, B. Stiller, M. Langer and R. Arnold. "4D-MR flow analysis in patients after repair for tetralogy of Fallot". Eur Radiol, 21, 1651-1657, 2011.
11 C. J. Francois, S. Srinivasan, M. L. Schiebler, S. B. Reeder, E. Niespodzany, B. R. Landgraf, O. Wieben and A. Frydrychowicz. "4D cardiovascular magnetic resonance velocity mapping of alterations of right heart flow patterns and main pulmonary artery hemodynamics in tetralogy of Fallot". J Cardiovasc Magn Reson, 14, 16, 2012.
12 D. Hirtler, J. Garcia, A. J. Barker and J. Geiger. "Assessment of intracardiac flow and vorticity in the right heart of patients after repair of tetralogy of Fallot by flow-sensitive 4D MRI". Eur Radiol, 26, 3598-3607, 2016.
13 P. Bachler, I. Valverde, N. Pinochet, S. Nordmeyer, T. Kuehne, G. Crelier, C. Tejos, P. Irarrazaval, P. Beerbaum and S. Uribe. "Caval blood flow distribution in patients with Fontan circulation: quantification by using particle traces from 4D flow MR imaging". Radiology, 267, 67-75, 2013.
14 J. Zajac, J. Eriksson, P. Dyverfeldt, A. F. Bolger, T. Ebbers and C. J. Carlhall. "Turbulent kinetic energy in normal and myopathic left ventricles". J Magn Reson Imaging, 41, 1021-1029, 2015.
15 P. Sjoberg, S. Bidhult, J. Bock, E. Heiberg, H. Arheden, R. Gustafsson, S. Nozohoor and M. Carlsson. "Disturbed left and right ventricular kinetic energy in patients with repaired tetralogy of Fallot: pathophysiological insights using 4D-flow MRI". Eur Radiol, 2018.
16 V. P. Kamphuis, A. A. W. Roest, J. J. M. Westenberg and M. S. M. Elbaz. "Biventricular vortex ring formation corresponds to regions of highest intraventricular viscous energy loss in a Fontan patient: analysis by 4D Flow MRI". Int J Cardiovasc Imaging, 34, 441-442, 2018.
17 J. Wong, R. Chabiniok, S. M. Tibby, K. Pushparajah, E. Sammut, D. S. Celermajer, D. Giese, T. Hussain, G. F. Greil, T. Schaeffter and R. Razavi. "Exploring kinetic energy as a new marker of cardiac function in the single ventricle circulation". J Appl Physiol (1985), 2018.
18 A. Tandon, S. Hashemi, W. J. Parks, M. S. Kelleman, D. Sallee and T. C. Slesnick. "Improved high-resolution pediatric vascular cardiovascular magnetic resonance with gadofosveset-enhanced 3D respiratory navigated, inversion recovery prepared gradient echo readout imaging compared to 3D balanced steady-state free precession readout imaging". J Cardiovasc Magn Reson, 18, 74, 2016.
19 L. M. Lai, J. Y. Cheng, M. T. Alley, T. Zhang, M. Lustig and S. S. Vasanawala. "Feasibility of ferumoxytol-enhanced neonatal and young infant cardiac MRI without general anesthesia". J Magn Reson Imaging, 45, 1407-1418, 2017.

Contact

Timothy C. Slesnick, M.D.
Director, Cardiac MRI
Children's Healthcare of Atlanta
Associate Professor
Department of Pediatrics
Emory University School of Medicine
1405 Clifton Road North East
Atlanta, GA 30322
USA
Tel: +1 404-256-2593
SlesnickT@kidsheart.com